Bulletin of Earth Sciences of Thailand

Evolution of Precursory Seismic Quiescence of the M_w-6.8 Nam Ma Earthquake, Thailand-Myanmar Borders

Prayot Puangjaktha* and Santi Pailoplee

Earthquake and Tectonic Geology Research Unit (EATGRU), Department of Geology, Faculty of Science, Chulalongkorn University, Bangkok 10330, Thailand
** Corresponding author E-mail: Puangjaktha.P@gmail.com*

Abstract

We analyzed the evolution of the seismicity pattern related with the Nam Ma earthquake (M_W = 6.8) by using the statistical seismology method *RTL* (Region–Time–Length) algorithm to the seismicity data of the International Seismological Centre (ISC), recorded during 1969 - 2014. With using appropriate characteristic *RTL* parameter r_0 = 90 km, t_0 = 1.5 year and the minimum number of event (n) = 30, the retrospective assessment of *RTL* algorithm along Thailand-Laos-Myanmar borders have implied that the seismicity pattern changes before the main shock of earthquake. To illustrate clearly the evolution of seismicity pattern, the spatial distribution map were sliced by the time interval every 0.25 year before and after the Nam Ma earthquake. Following the quiescence stage, the anomalous area appeared corresponding to the epicenter of an earthquake. Hence, considering the seismic quiescence as precursory seismicity may provide beneficial information for understanding the process of strong earthquakes and evaluating the hazard or risk alarm.

Keywords: Earthquake Catalogue; Precursory Seismic Quiescence; *RTL* Algorithm; Earthquake Forecasting; Thailand-Myanmar Borders.

1. Introduction

The tectonic setting of Thailand-Laos-Myanmar borders is situated in a widespread intraplate activity where the inland seismologenic faults are dominant. Base on earthquake catalogue available from the International Seismological Centre (ISC) since 1969, there are 9 strong earthquakes ($M_w \geq 6.0$) occurred in this area. Moreover, the previous study about this region applied *b*-value of the frequency-magnitude distribution model (FMD; Gutenberg and Richter, 1944) for investigating precursory seismicity. The results indicated good correlation between *b*-value and the subsequent large earthquakes (Pailoplee et al., 2013). The low *b*-value area represent to the high stress zone that it related with an occurrence of impending earthquake. Thus, this area is one of the high level of seismic activity zone, (Fig. 1).

Nowadays, there are various assumptions created for finding earthquake precursor. However, several significant researches sustained the hypothesis that sei smic quiescence precedes large earthquake (Katsumata, 2011). Therefore in order to find out the earthquake precursor, a large number of statistical method were demonstrated for earthquake forecasting (Tiampo and Shcherbakov, 2012) such as

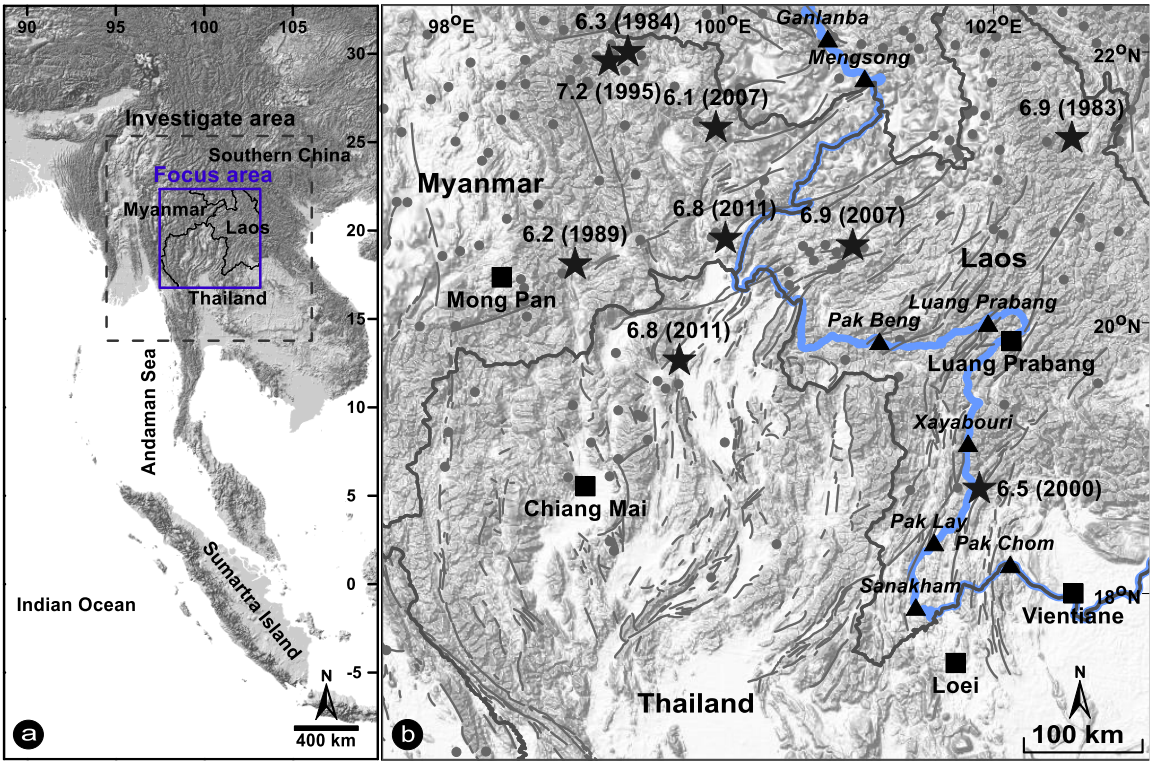

Fig. 1. (a) Map of Thailand and neighborhood countries showing the area which the earthquake sources were investigated (outer box with dash line) and the focused area for illustrating seismic quiescence patterns (inner box with blue line). (b) Map showing the epicenters of completeness seismicity catalogue (grey dots, with $m_b \geq 3.7$) and strong earthquake's epicenter (black star, with $M_w \geq 6.0$) distribution along Thailand-Laos-Myanmar borders during the period 1982 and 2012. The fault lines, Mae Kong River, hydro-power dams and major cities were shown by grey line, thick blue line, black triangles and black squares, respectively.

Z-value (Wiemer and Wyss, 1994), Pattern Informatics (PI) index (Holliday et al., 2006), Accelerating Moment Release (AMR) (Ben-Zion and Lyakhovsky, 2002), and the Load–Unload Response Ration (LURR) (Yin et al., 1995), etc.

Among statistical approaches mentioned above, the *RTL* algorithm is another success forecasting techniques to quantify relative seismic quiescence and seismic activation. It was initially tested at Kamchatka, Russia. The result found that the strong earthquakes in Kamchatka with magnitude M > 7.0 had been preceded by seismic quiescence stage started 1.5 – 3.5 years and lasted 1.0 – 2.5 years, quiescence stage changes to be activation stage with a duration varying from 0.5 – 1.5 years (Sobolev and Tyupkin, 1997). Then, many seismologists had been published the researches about this algorithm, for example, Huang et al. (2001) discovered quiescence stage started in 1993 and got to the minimum in May 1994, following by activation stage about 7 months before the January 17, 1995 Kobe earthquake (M = 6.8), Japan. Thereafter, Huang and Sobolev (2002) found the seismic quiescence started in 1995 and attained its minimum in October 1996, after that the subsequent stage of seismic activation stage started with a period about 8 months before the January 28, 2000 of the Nemuro Peninsula earthquake (M = 6.8), Japan. After that Chen and Wu(2006)

observed seismic quiescence started 2 years before the September 21, 1999 Chi Chi earthquake (M_w = 7.6), Taiwan. Minan and Givovambattista (2008) perceive quiescence pattern began 2.4 year before the September 26, 1997 Umbria-Marche earthquake (M = 4.8), Italy. Shashidhar et al. (2010) found seismic quiescence started 0.6 year before the September 16, 2008 Koyna region (M_w = 5), Western India. Gambino et al. (2014) discovered seismic quiescence period started 1.25 year before the August 16, 2010 Aeolian Archipelago (M_w = 4.8), Italy; and etc. Nevertheless, due to a few study with seismic activation, we, therefore focus to investigate the evolution about seismic quiescence stage in the vicinity of Thailand-Myanmar border by using the *RTL* algorithm.

2. *RTL* algorithm

The concept about the *RTL* algorithm has been suggested by Sobolev and Tyupkin (1997; 1999), the basic hypothesis based on three dimensionless parameters called R (interested region), T (time) and L (rupture length) that we can defined as equations (1) - (3).

$$R(x,y,z,t)=\left[\sum_{i=1}^{n}\exp\left(-\frac{r_i}{r_0}\right)-R_{bg}(x,y,z,t)\right] \quad (1)$$

$$T(x,y,z,t)=\left[\sum_{i=1}^{n}\exp\left(-\frac{t-t_i}{t_0}\right)-T_{bg}(x,y,z,t)\right] \quad (2)$$

$$L(x,y,z,t)=\left[\sum_{i=1}^{n}\exp\left(-\frac{l_i}{r_i}\right)-L_{bg}(x,y,z,t)\right] \quad (3)$$

Where (x,y,z,t) specifies the focused location and time; r_i is the range from the interested location of (x,y,z) to the i^{th} earthquake's epicenter; t_i is the incident time of the i^{th} earthquake, r_0 and t_0 are the characteristic distance and characteristic time-span of interested region; l_i is the rupture length of the i^{th} considering earthquake, converted by using the empirical relationship among magnitude and rupture length as defined in equation (4), M is magnitude of earthquake and SRL indicate surface rupture length (Wells and Coppersmith, 1994); $R_{bg}(x,y,z,t)$, $T_{bg}(x,y,z,t)$ and $L_{bg}(x,y,z,t)$ are the background values of $R(x,y,z,t)$, $T(x,y,z,t)$ and $L(x,y,z,t)$, respectively; n is the number of events with RTL parameters satisfying some criteria. e.g. $M_i \geq M_{min}$ (M_i is the magnitude of the i^{th} earthquake and M_{min} is the cut-off magnitude assuring the completeness of earthquake data), $2r_0 = R_{max} \geq r_i$ and $2t_0 = t_{max} \geq t - t_i$; and $V_{RTL}(x,y,z,t)$ is the RTL function.

$$M = 5.08 + 1.16 * \log(SRL) \quad (4)$$

Afterward, we bounded the variation range of the numerical values of RTL function in [-1, 1] before plotted the temporal RTL curves by using normalized equation as equation (5) (Jiang et al., 2004). The result of normalized RTL function can insulate the earthquake behavior in the interested region that $V_{RTL} = 0$ represented normal earthquake activity, $V_{RTL} > 0$ represented seismic activation and $V_{RTL} < 0$ represented seismic quiescence.

$$V_{RTL}(x,y,z,t)=\frac{R(x,y,z,t)}{R(x,y,z,t)_{\max}}\bullet\frac{T(x,y,z,t)}{T(x,y,z,t)_{\max}}\bullet\frac{L(x,y,z,t)}{L(x,y,z,t)_{\max}} \quad (5)$$

Eventually, to quantify the seismic quiescence stage, we used $Q(x, y, z, t_1, t_2)$ function or Q-parameter developed by Huang (2004) for average the *RTL* values at the position (x, y, z) during interested time window [t_1, t_2]. The $Q(x, y, z, t_1, t_2)$ function is defined as equation (6).

$$Q(x,y,z,t_1,t_2) = \left\lfloor \sum_{i=1}^{n} V_{RTL}(x,y,z,t_i) \right\rfloor \quad (6)$$

Where t_i is the focus time in the time window [t_1, t_2], $V_{RTL}(x, y, z, t_i)$ is the normalized *RTL* values calculated as the product of the equation (5) applying the earthquakes in cylindrical volume, n is the minimum number of earthquake data for computing V_{RTL} values. In this study, the Q-parameter at each grid nodes is computed at a bin (time step) of 14 days available in [t_1, t_2]. A sketch of the introduced algorithms is given in Fig. 2.

3. Data set and completeness

In this study, we used the earthquake catalogue from the International Seismological Center (ISC). The earthquakes occurred along the Thailand-Laos-Myanmar borders (13.77° – 25.35°E and 94.48° – 106.07°N) during the period from 1964 to 2013 will be investigated. However, the results of spatial distribution was cropped out to the latitude 16.76° – 22.30°E and longitude 97.48° - 103.16° for cut-off the uncalculated nodes. The different magnitude types were converted to body wave magnitude (m_b) using the relationships contributed empirically by the Global Centroid Moment Tensor data available along the Thailand-Laos-Myanmar borders. In order to find the com-

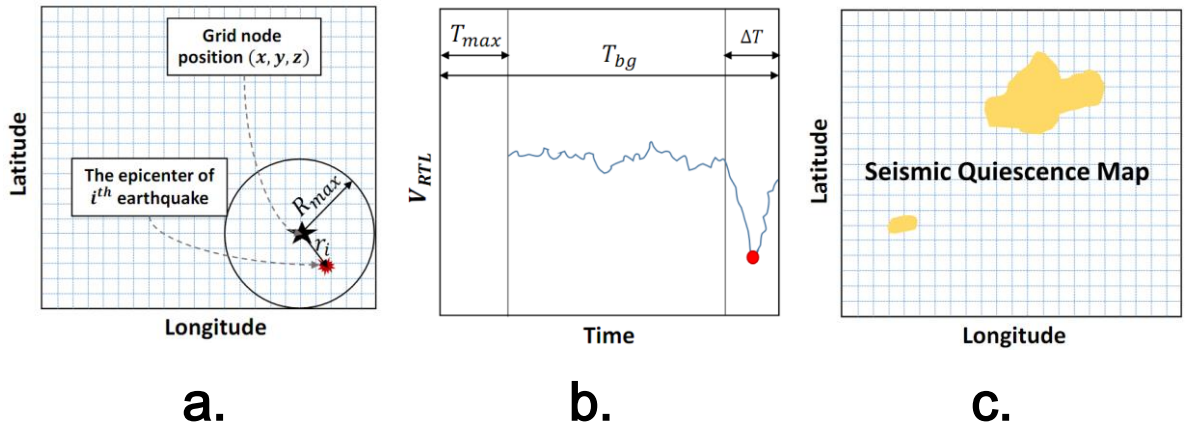

Fig. 2. The diagrams for evaluating the spatial distribution of seismic quiescence at the position (x, y, z) showing (a) the map shows the threshold of framing area by R_{max} and the distance from selected grid node to the position of i^{th} earthquake's epicenter. (b) The diagram shows the curve of V_{RTL} at each grid node considered and the minimum V_{RTL} (marked by a red circle), where T_{bg} is the total background time for calculating *RTL* algorithm, ΔT is the period of time-span for investigating seismic quiescence, T_{max} is the limited range of time-span. (c) The cartoon of seismic quiescence map. The shadowed area represented the seismic quiescence of the study area in the focus time interval.

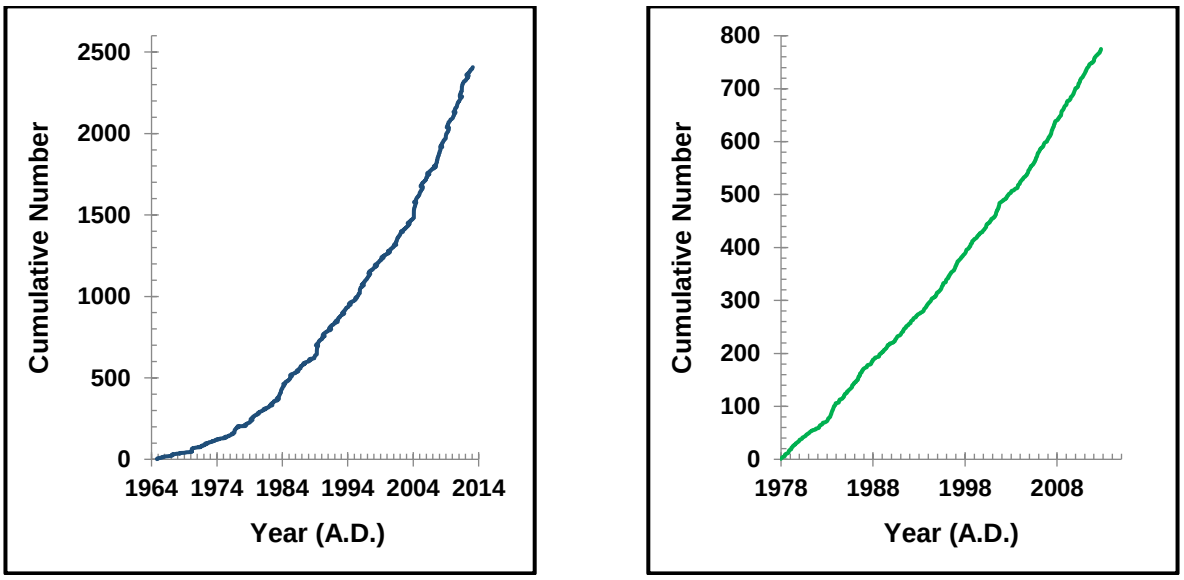

a. **b.**

Fig. 3. Cumulative number showing the constant rates of a) seismicity detected from ISC during period 1964-2013 b) the completeness earthquake data after catalogue improvement during November 29, 1977 and September 11, 2012.

pleteness we applied the procedure given by Gardner and Knopoff (1974) to eliminate the foreshock and the aftershock. The completeness of earthquake detecting technique was also checked using the power-law FMD. Based on the presumption of Entire-magnitude Range (Woessner and Wiemer, 2005), we found that the magnitude of completeness (M_{min}) = 3.7 m_b during November 29, 1977 and September 11, 2012 can cover most parts of the Thailand-Laos-Myanmar borders (Fig. 3a).

Then, using the GENAS algorithm (Habermann, 1983; 1987) to take out the harmonic main shock of the magnitude completeness. The linear line of cumulative number of earthquakes as explicated in Fig. 2b shows that no apparent man-made activity in the bulk seismicity rate as mentioned by Wyss (1991) and Zuniga and Wiemer (1999). Therefore, we decided to use all remained 775 main shocks with $m_b \geq 3.7$ recorded during 1969 and 2012 in this *RTL* investigation (Fig. 3b).

4. Results

We analyzed the temporal variations of the *RTL* values (in unit of standard deviation, σ) of the Nam Ma earthquake (M_w= 6.8). At the first, the characteristic parameters, i.e., R_{max} and T_{max} were varied according to that propose in the previous works. Then in each grid nodes, the *RTL* algorithm were evaluated temporally in every 14 day starting at the beginning through the occurrence time of earthquake considered. The spatial distributions of seismic quiescence were also analyzed using the method mentioned above. In this study, there are a number of variable *RTL* parameters. However, we attempted different values for the suitable characteristic parameters, the most fitting characteristic parameters is chosen retrospectively throughout the observation, temporal and spatial investigation. As a result, it is indicated that the condition of characteristic distance r_0 = 90 (R_{max} = 180 km) and characteristic time-span t_0 = 1.5

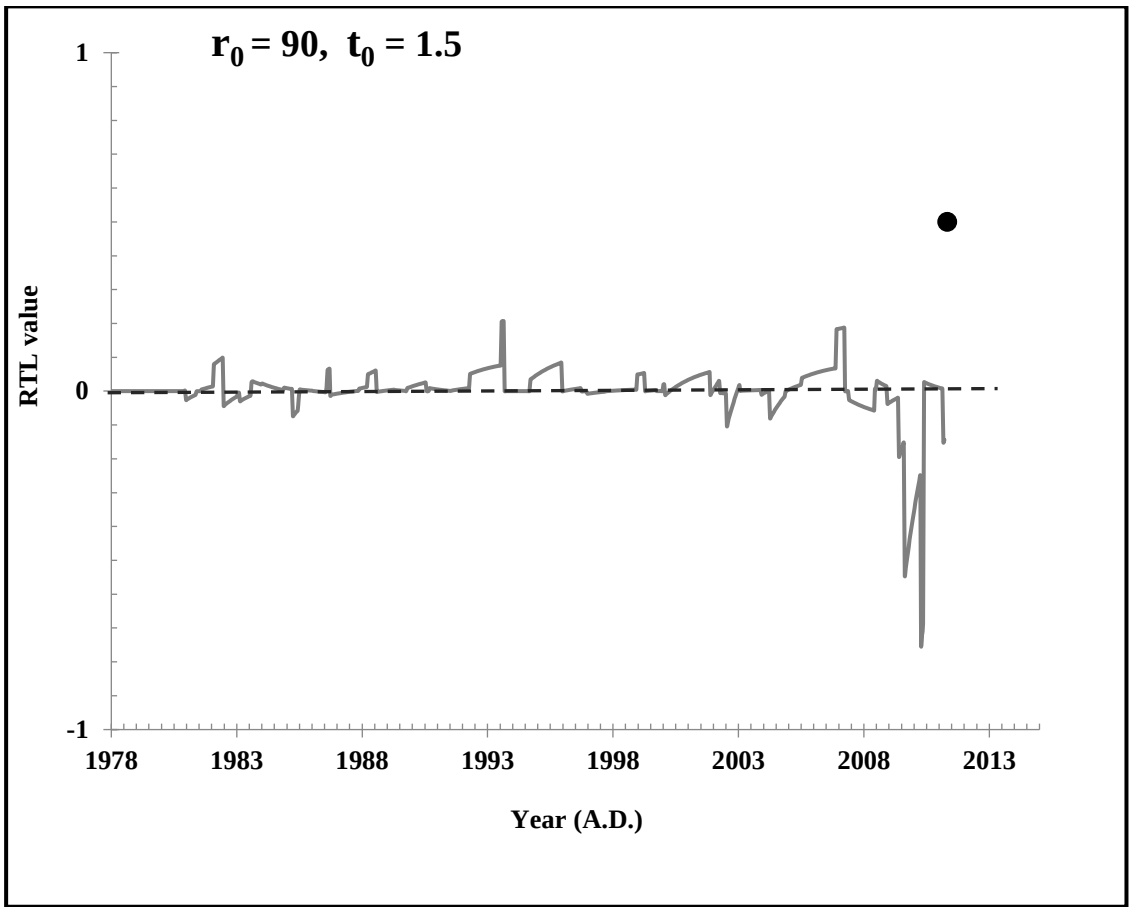

Fig. 4. Temporal variation of *RTL* values at the epicenter of the Nam Ma earthquake (longitude 99.92 and latitude 20.63) during 1978 and 2012, estimation with characteristic parameter r_0 = 90, t_0 = 1.5. The black circle indicates the occurrence time of the Nam Ma earthquake on March 24, 2011.

(T_{max} = 3 years) including minimum number of calculated earthquake events (*n*) = 30 successful to find out the anomalous seismic activity. At the epicenter of the Nam Ma earthquake (longitude 99.92 and latitude 20.63), the normalized *RTL* values curve started decreasing at 2009.40 (1.83 years) and reached 2010.28 with the minimum *RTL* value is - 0.75, after that, the curve returned to normal in short time follow with the occurrence of the Nam Ma earthquake main shock (Fig. 4).

Furthermore, the spatial distribution of this condition shows the *RTL* anomalies corresponding to the epicenter of the March 24, 2011 Nam Ma earthquake (Fig. 4). In this study, we compared the spatial map with various conditions. The introduced condition above seem to show the anomaly area better than others conditions. However, when considering the retrospective temporal variation thoroughly, the March 24, 2011 Nam Ma earthquake did not occur immediately after the quiescence stage. The seismicity pattern return to background stage (*RTL* = 0) around 9 month before the Nam Ma earthquake occurred. Hence, we generated quiescence map every 3 months during July 1, 2009 and September 31, 2012 for understanding the develop of seismicity patterns in each time step and observed the evolution of precursory seismicity patterns before and after the main shock of the Nam Ma earthquake. We found the results can classify as 3 phases, i.e., i) during quiescence stage (Fig. 6), ii) after

quiescence phase (Fig. 7), and iii) after earthquake occurrence (Fig. 8).

The first phase, we noticed the *RTL* anomalies covered over 300 km^2 in the vicinity of northern Thailand, eastern Myanmar, western Laos including southern China (Fig. 6). The mentioned anomalies illustrate around 1 year time-span although the minor and the major earthquake occurred among its. However at the second phase, anomalous area mostly disappear immediately after the end of quiescence stage (Fig. 7). Then after the Nam Ma earthquake, the anomalous region at the epicenter was clearly disappear and start develop dimly at the neighbor areas, once of them subsequent with the March 5, 2014 Mae Lao earthquake (M_w= 6.2), Thailand (Fig. 8).

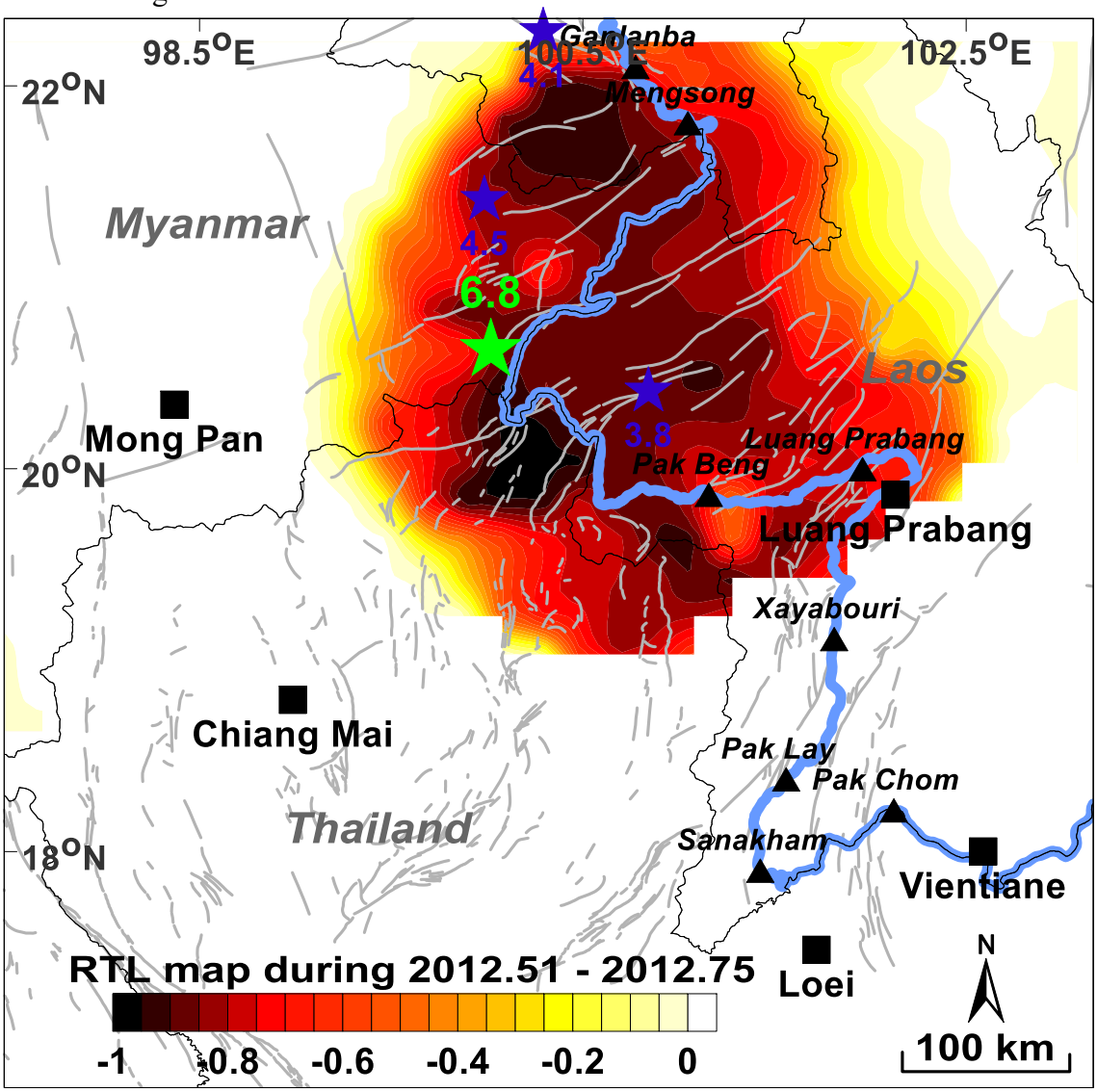

Fig. 5. Spatial distribution of *RTL* values along Thailand-Laos-Myanmar borders during the observed seismic quiescence stage with the minimum of *RTL* value before main shock (2010.28 – 2010.36). The shadowed zone indicates quiescence area, blue star implies the epicenter of minor and light earthquakes with body-wave magnitude (m_b) that they occurred during the time period of this map, and green star shows the Nam Ma earthquake.

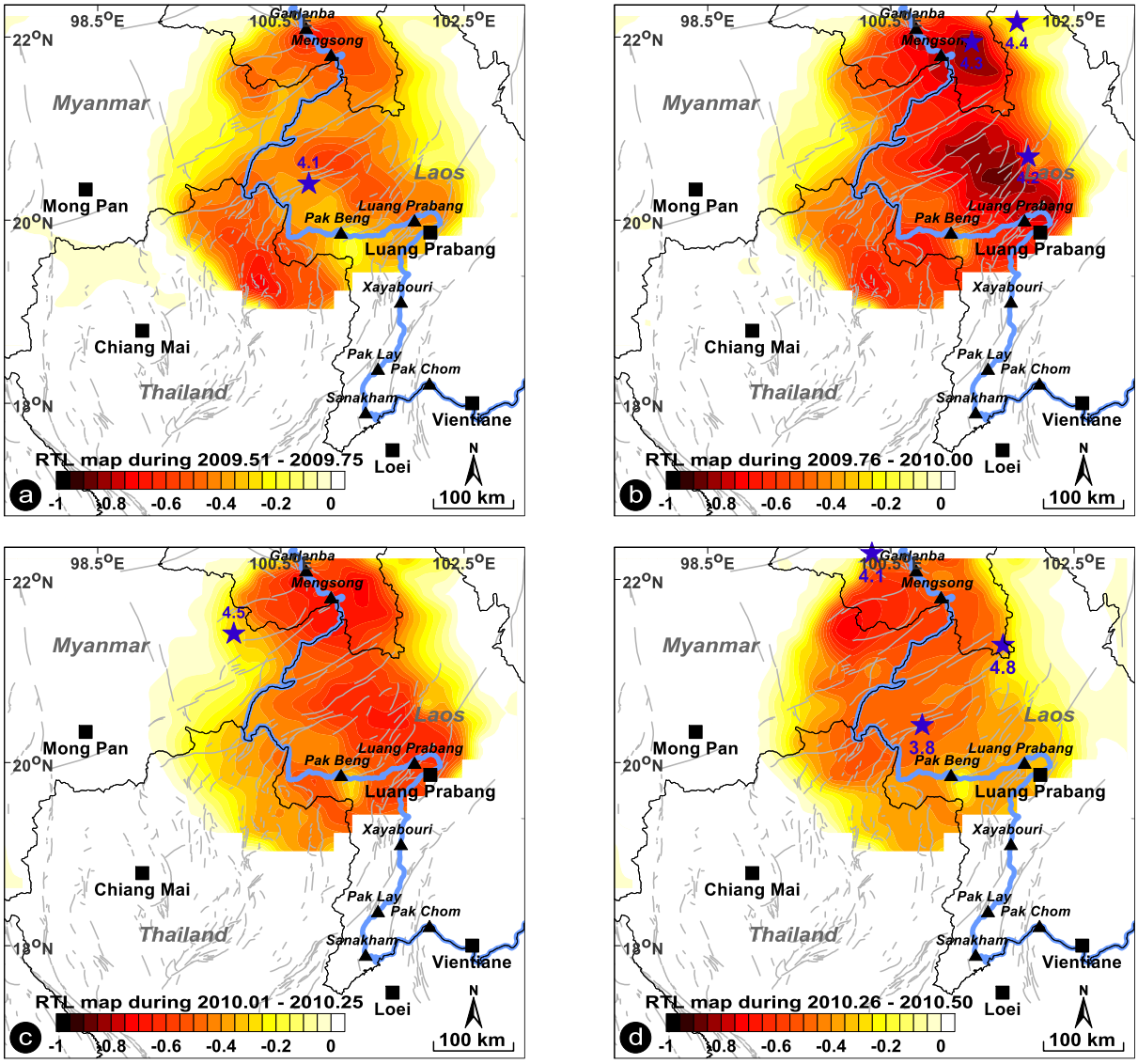

Fig. 6. Spatial distribution of *RTL* values indicate the evolution of seismic quiescence in quiescence phase during (a) July 1, 2009 – September 31, 2009 (b) October 1, 2009 – December 31, 2009 (c) January 1, 2010 – March 31, 2010 (d) April 1, 2010 - June 31, 2010. Shadowed area imply the zone of negative *RTL* values, blue star represent implies the epicenter of minor and light earthquakes with body-wave magnitude (m_b) that they occurred during each map.

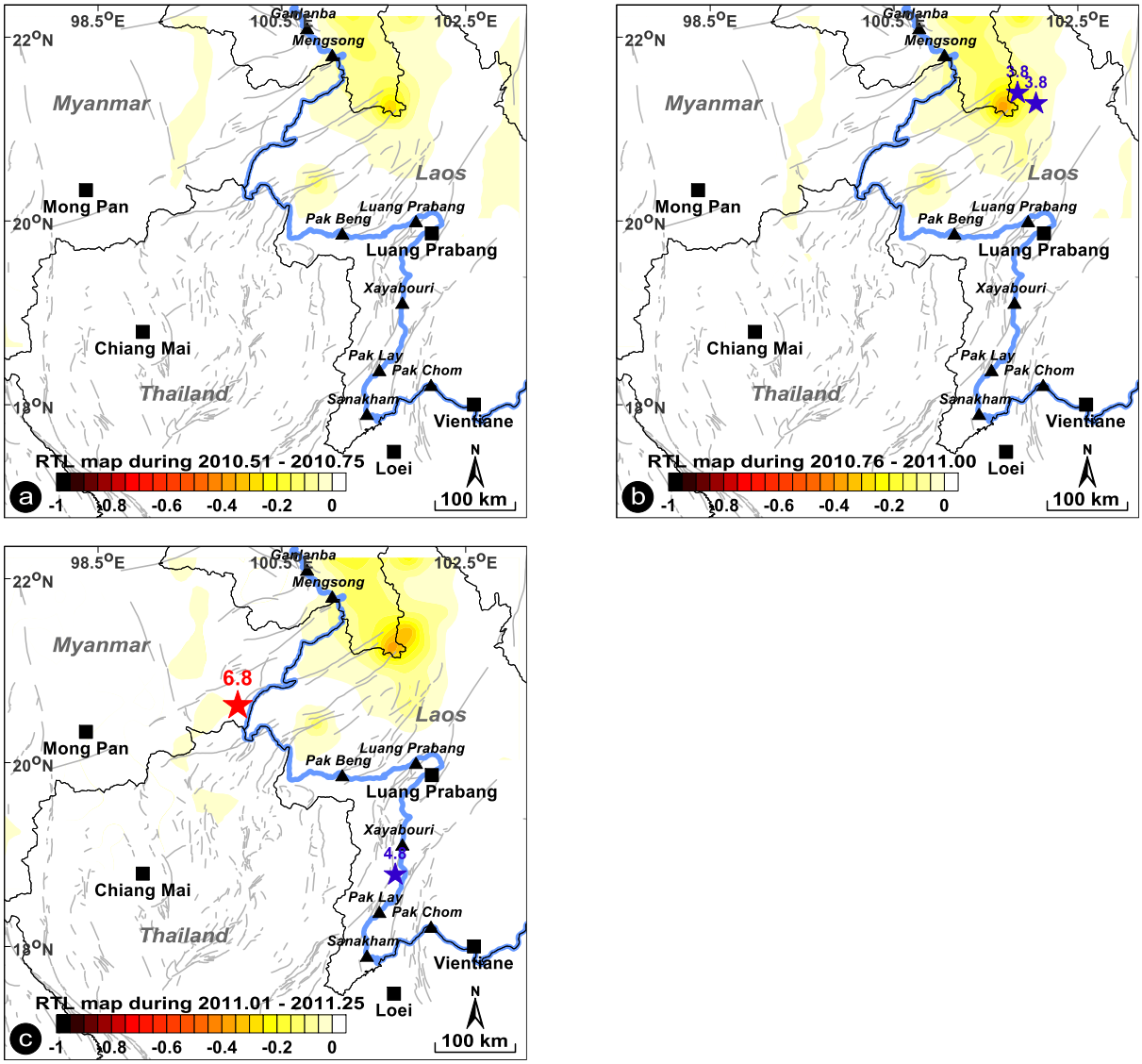

Fig. 7. Spatial distribution of *RTL* values indicate the evolution of seismic quiescence after quiescence stage, map during (a) July 1, 2010 – September 31, 2010 (b) October 1, 2010 – December 31, 2010 (c) January 1, 2011 – March 31, 2011. Shadowed area imply the zone of negative *RTL* values, blue star represent implies the epicenter of minor and light earthquakes with body-wave magnitude (m_b) that they occurred during each map, Red star shows the epicenter of the Nam Ma earthquake.

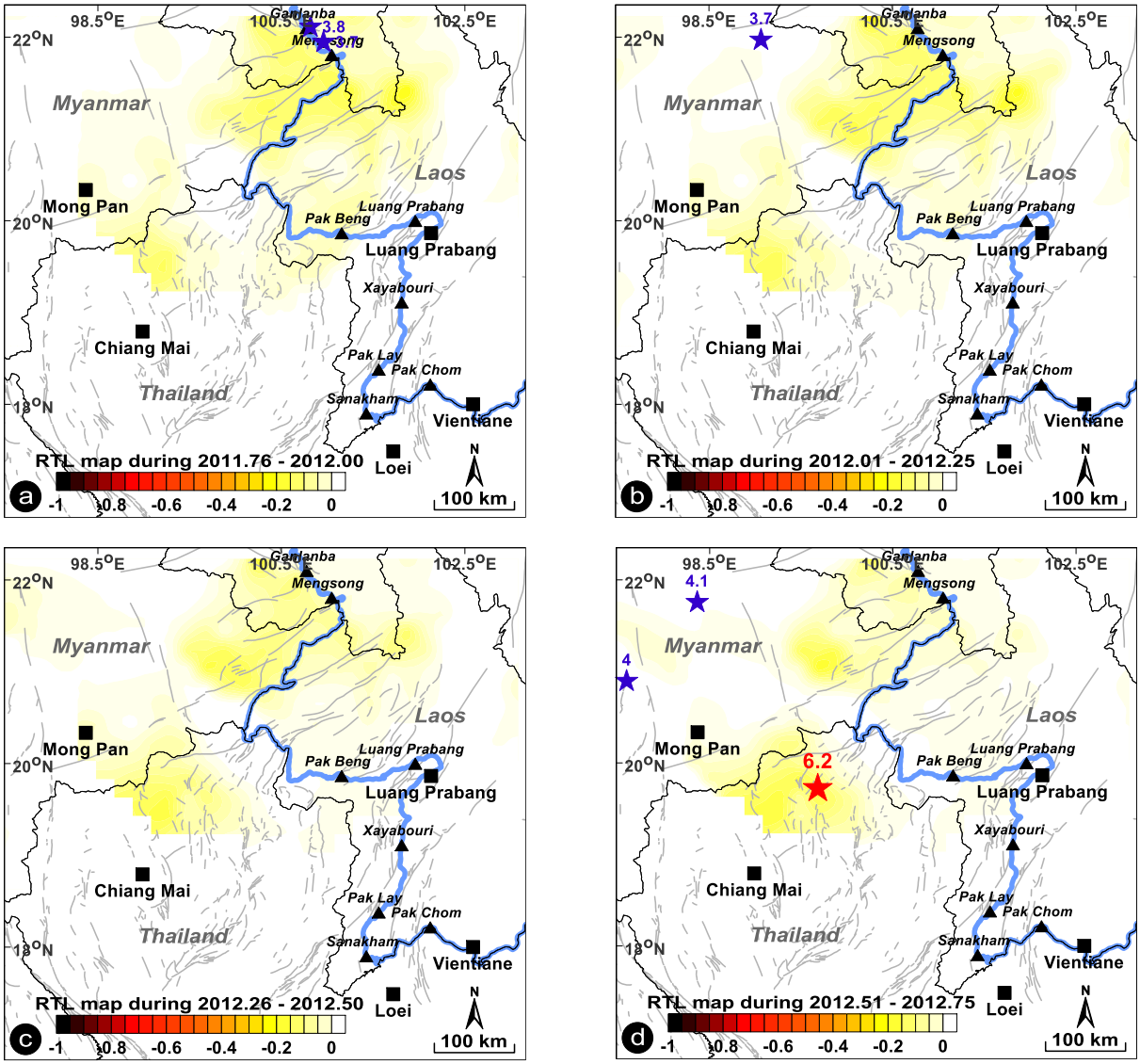

Fig. 8. Spatial distribution of *RTL* values indicate the evolution of seismic quiescence after quiescence stage, map during (a) October 1, 2011 – December 31, 2011 (b) January 1, 2012 – March 31, 2012 (c) April 1, 2012 – June 31, 2012 (d) July 1, 2012 - September 31, 2012. Shadowed area imply the zone of negative *RTL* values, green star represent implies the epicenter of minor and light earthquakes with body-wave magnitude (m_b) that they occurred during each map, Red star shows the epicenter of the March 5, 2014 Mae Lao earthquake, Thailand.

5. Discussions

5.1 Influence of characteristic *RTL* parameters

Base on Huang (2004) the characteristic parameters (r_0 and t_0) effect directly to the *RTL* investigation. In order to observe such changes, we repeated the *RTL* calculations by applying the different characteristic parameters. We used characteristic distance r_0 = 90 (R_{max} = 180 km), characteristic time-span t_0 = 1.5 (T_{max} = 3 years) in our analysis, determined by the criteria of previous researched about *RTL* algorithm and the corresponding between characteristic parameter and retrospective results. Subsequently, we plot the results of *RTL* curves at each conditions for considering the suitable characteristic parameter (Fig. 9). Furthermore, we also compute the correlation coefficient with the different characteristic *RTL* parameters. The statistical analysis implied that all the conditions listed in Table 1 correlated at a significance of 0.05. Hence, this can support that the anomaly of seismic quiescence, which was detected before the Nam Ma earthquake, is not an artificial anomaly due to the selections of characteristic *RTL* parameters.

5.2 Evolution of seismic quiescence stage

The temporal variation shows seismic quiescence stage of the Nam Ma earthquake started in the middle of June 2009 (1.83 years before main shock) and decreasing until the beginning of April 2010 with minimum *RTL* value. However, the earthquake did not occur immediately in this stage. Afterward, the result shows the *RTL* curve increase gradually and returned to the normal stage about 9 months before the main shock. A homologous time delay after the quiescence stage was also informed by previous *RTL* research such as the study of December 5, 1997 northern Gulf of Kamchatka earthquake (M = 7.7), Russia (Sobolev and Tyupkin, 1999), Sobolev and Tyupkin reported that the northern Gulf of Kamchatka have seismic quiescence stage, following with seismic activation stage and time delay about 1.5 years subsequent the end of the seismic activation phase; the January 28, 2000 Nemuro Peninsula earthquake (M_w = 6.8), Japan (Huang and Sobolev, 2002), Huang and Sobolev detected seismic quiescence started in 1995 with its duration time about 1.5 years until the end of 1996, after that, the seismic activation stage appeared with the duration time about 0.7 year and returned to the normal stage about 2.5 years before the January 28, 2000 Nemuro Peninsula earthquake occur; the August 16, 2010 Aeolian Archipelago (M_w = 4.8), Italy (Gambino et al., 2014), Gambino et al. (2014) discovered seismic quiescence period started about 1.25 years before the earthquake with its duration approximately about 6 - 7 months and returned to the normal stage without an seismic activation stage, time delayed about 7 months before the August 16, 2010 Aeolian Archipelago earthquake, Italy, and etc.

Table 1. Correlation of *RTL* values between different characteristic parameters r_0 and t_0. Case (A) shows the suitable values of independent characteristic parameters that we using for investigate precursory seismicity changes before the Nam Ma earthquake, (B) the different characteristic *RTL* parameters that we using for comparison with suitable condition.

cases	A	r_0 = 90 km, t_0 = 1.5 years			
	B	r_0 = 65 km	r_0 = 115 km	t_0 = 1.25 Yrs.	t_0 = 1.75 Yrs.
Correlation between A and B		0.96	0.96	0.67	0.74

Therefore, the investigation of seismicity pattern changes may provide useful information for forecasting future earthquake. Nevertheless, the existence phase of time delay which introduced above makes it hardly to evaluate and determine the occurrence time accurately in short-term earthquake forecasting.

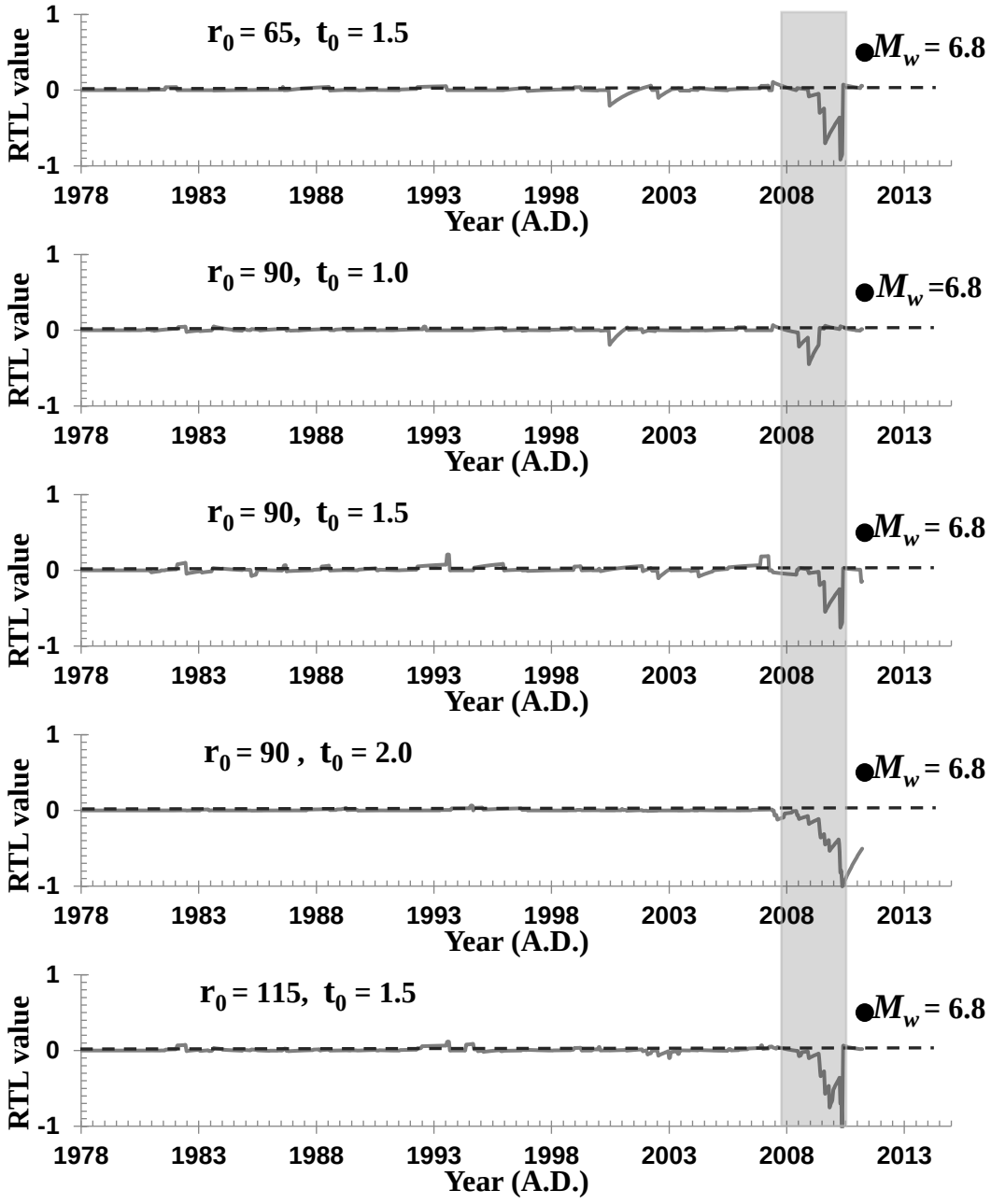

Fig. 9. Temporal variation of *RTL* values at the epicenter of the Nam Ma earthquake (longitude 99.92 and latitude 20.63) during 1978 and 2012, estimation with different values of characteristic *RTL* parameters reported in each graphs. The examples of results indicated the different conditions effected to the different *RTL* curves. The grey strip denoted the time span of *RTL* seismic quiescence. However, some conditions generated the rather similarly result. Therefore, it's necessary to determine the suitable factors base on the criteria of previous study about *RTL* algorithm and the relation between characteristic parameters and retrospective results, both of temporal and spatial investigation.

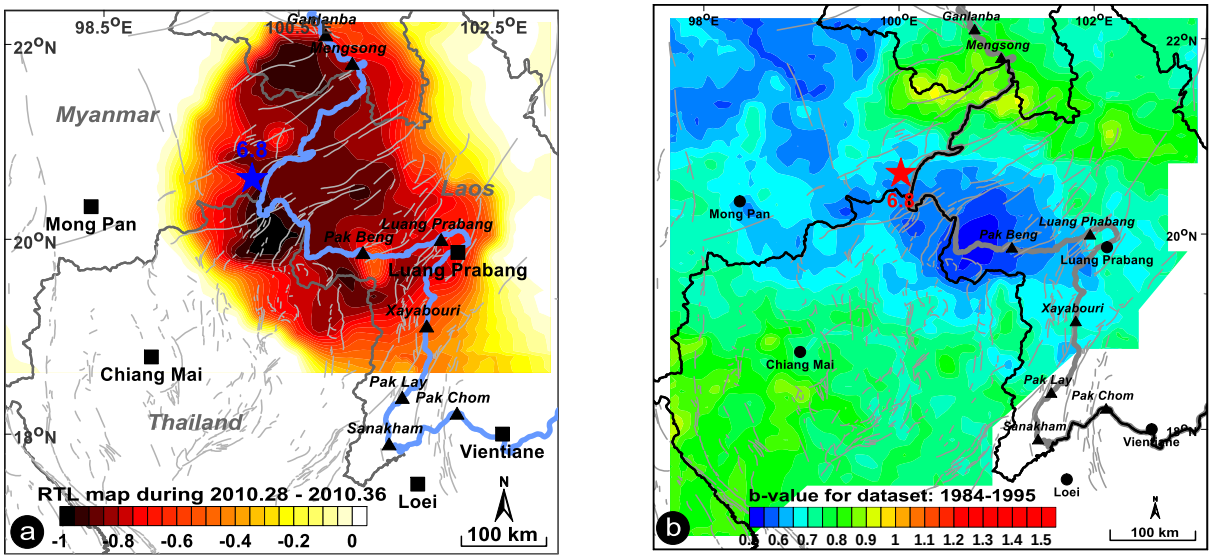

Fig. 10. Spatial distribution of a) *RTL* values during 2010.28 – 2010.36 and b) *b*-value using the seismicity data recorded during 1984 – 2010 (Pailoplee et al., 2013).

5.3 Prospective area of the upcom-ing earthquake source.

In order to constrain the *RTL* evaluated in this study (Fig. 10a), the obtain results were compared with *b*-value of FMD (Pailoplee et al., 2013). It is revealed that at the same duration time of 2010, the area showing comparatively low of *RTL* (this study) quite conform to the comparatively low of low *b* (Fig. 10b; Pailoplee et al., 2013). Seismotectonically, the lower *RTL* imply the higher of seismic quiescence. Meanwhile, the lower b of FMD relate empirically to higher stress accumulated. Therefore, it is interpreted that the low-*RTL* area mentioned above act as presently high stress area and the earthquake activity are still quiescence.

6. Conclusion and Recommendation

We analyzed the evolution of seismicity pattern changes before the Nam Ma earthquake (M_w= 6.8) by using the *RTL* (Region-Time-Length) algorithm with the condition of characteristic distance r_0 = 90 (R_{max} = 180 km) and characteristic time-span t_0 = 1.5 (T_{max} = 3 years) including minimum number of calculated earthquake events (n) = 30 to the seismicity catalogue of the International Seismological Center (ISC). We found the main shock occurred 1 year after the end of quiescence stage, similarly with previous *RTL* studies. Afterward, the evaluating with the different conditions, it is indicated that the anomalous *RTL* region obtained here are accurate according to the reliable high coefficient of correlations. Moreover, after the Nam Ma earthquake was posed, we detected the development of seismic quiescence area before the March 5, 2014 Mae Lao earthquake, Thailand occurred. Therefore with the suitable r_0 = 90 and t_0 = 1.5, we can conclude that *RTL* algorithm can use to be one of the precursory seismicity pattern changes along Thailand-Laos-Myanmar borders. However according to various steps of *RTL* maps obtained in this study, it is noticeable that the *RTL* changes sensitively with the short time period. Therefore in order to investigate accurately the seismicity changes prior the strong earthquake, the investigations of *RTL* algorithm including the others method should be monitor frequently. In addition according to the limitation of seismicity data used in this study, i.e., only the International Seismolo-

gical Center (ISC), the result obtained in this study were therefore scoped in specific short time period. The more seismicity data, the more accuracy of *RTL* investigation in further.

7. Acknowledgements

This research was supported by the Ratchadapiseksomphot Endowment Fund 2015 of Chulalongkorn University (WCU-58-021-CC). Thanks are also extended to T. Pailoplee for the preparation of the draft manuscript. I acknowledge thoughtful comments and suggestions by the editors and anonymous reviewers that enhanced the quality of this manuscript significantly.

8. References

Ben-Zion, Y., Lyakhovsky, V., 2002. Accelerated seismic release and related aspects of seismicity patterns on earthquake faults. *Pure and Applied Geophysics*; 159, 2385–2412.

Chen, C., Wu, Y., 2006. An improved region-time-length algorithm applied to the 1999 Chi-Chi, Taiwan earthquake. *Geophysical Journal International*; 166, 144-147.

Gambino, S., Laudani, L., Magiagle, S., 2014. Seismicity Pattern Changes before the *M* = 4.8 Aeolian Archipelago (Italy) Earthquake of August 16, 2010. *The Scientific World Journal Volume 2014*; 531212.

Gardner, J.K., Knopoff, L., 1974. Is the sequence of earthquakes in Southern California, with aftershocks removed, Poissonian?. *Bulletin of the Seismological Society of America*; 64(1), 363–367.

Gutenberg, B., Richter, C.F., 1944. Frequency of earthquakes in California. *Bulletin of the Seismological Society of America*; 34, 185-188.

Habermann, R.E., 1983. Teleseismic detection in the Aleutian Island Arc. *Journal of Geophysical Research*; 88, 5056-5064.

Habermann, R.E., 1987. Man-made changes of seismicity rates. *Bulletin of the Seismological Society of America*; 77, 141–159.

Holliday, J.R., Rundle, J.B., Tiampo, K.F., Klein, W., Donnellan, A., 2006a. Systematic procedural and sensitivity analysis of the Pattern Informatics method for forecasting large MN5 earthquake events in southern California. *Pure and Applied Geophysics*; 10.1007/s00024-006-0131-1.

Huang, Q., Sobolev, G.A., Nagao, T., 2001. Characteristics of the seismic quiescence and activation patterns before the M=7.2 Kobe earthquake, January 17, 1995. *Tectonophysics*; 337(1-2), 99-116.

Huang, Q., Sobolev, G.A., 2002. Precursory seismicity changes associated with the Nemuro Peninsula earthquake, January 28, 2000. *Journal of Asian Earth Sciences*; 21(2), 135–146.

Huang, Q., 2004. Seismicity Pattern Changes Prior to Large Earthquakes – An Approach of the RTL algorithm. *TAO*; 15(3), 469-491.

Jiang, H.K., Hou, H.F., Zhou H.P., Zhou, C.Y., 2004. Region-time-length algorithm and its application to the study of intermediate-short term earthquake precursor in North China. *Acta Seismologica Sinica*; 17(2), 164-176.

Katsumata, K., 2011. A long-term seismic quiescence started 23 years before the 2011 off the Pacific coast of Tohoku Earthquake (*M* = 9.0). *Earth Planets Space*; 63, 709 – 712.

Mignan, A., Giovambattista R. D., 2008. Relationship between accelerating seismicity and quiescence, two precursors to large earthquakes. *Geophysical Research Letters*; 35, 10.1029/2008GL035024.

Pailoplee, S., Channarong, P., Chutakosikanon, V., 2013. Earthquake Activities in the Thailand-Laos-Myanmar borders: A Statistical Approach. *Terrestrial Atmospheric and Oceanic Sciences*; 24(4), 721-730.

Pailoplee, S., Surakiatchai, P., Charusiri, P., 2013. b-value Anomalies along the Northern Segment of Sumatra-Andaman Subduction Zone: Implication for the Upcoming Earthquakes. *Journal of Earthquake and Tsunami*; 7(3), 1350030-1-8.

Shashidhar, D., Kumar, N., Mallika, K., Gupta, H., 2010. Characteristics of seismicity patterns prior to the M~5 earthquakes in the Koyna Region, Western India – application of the RTL algorithm. *Episodes;* 33, 83 - 89.

Sobolev, G.A., Tyupkin, Y.S., 1997. Low-seismicity precursors of large earthquakes in Kamchatka. *Volcanology and Seismology*; 18, 433-446.

Sobolev, G.A., Tyupkin, Y.S., 1999. Precursory phases, seismicity precursors, and earthquake prediction in Kamchatka. *Volcanology and Seismology*; 20, 615-627.

Tiampo, K. R., Shcherbakov, R., 2012. Seismicity-based earthquake forecasting techniques: Ten years of progress. *Tectonophysics;* 522, 89–121.

Wells, D.L., Coppersmith, K.J., 1994. Updated empirical relationships among magnitude, rupture length, rupture area, and surface displacement. *Bulletin of the Seismological Society of America*; 84, 974-1002.

Wiemer, S., Wyss, M., 1994. Seismic quiescence before the Landers M=7.5 and Big Bear M=6.5 1992 earthquakes. *Bulletin of the Seismological Society of America*; 84, 900-916.

Woessner, J., Wiemer S., 2005. Assessing the Quality of Earthquake Catalogues: Estimating the Magnitude of Completeness and Its Uncertainty. *Bulletin of the Seismological Society of America*; 95(2), 684–698.

Wyss, M., 1991, Reporting history of the central Aleutians seismograph network and the quiescence preceding the 1986 Andreanof Island earthquake. *Bulletin of the Seismological Society of America*, 81, 1231–1254.

Yin, X.C., Chen, X.Z., Song, Z.P., Yin, C., 1995. A new approach to earthquake prediction: the Load/Unload Response Ratio (LURR) theory. *Pure and Applied Geophysics*; 145, 701–715.

Zuniga, F.R., Wiemer, S., 1999, Seismicity patterns: are they always related to natural causes?. *Pageoph*; 155, 713-726.